Unique secretory dynamics of tissue plasminogen activator and its modulation by plasminogen activator inhibitor-1 in vascular endothelial cells

Yuko Suzuki,[1] Hideo Mogami,[1] Hayato Ihara,[1] and Tetsumei Urano[1]

[1]Department of Physiology, Hamamatsu University School of Medicine, Hamamatsu, Japan

We analyzed the secretory dynamics of tissue plasminogen activator (tPA) in EA.hy926 cells, an established vascular endothelial cell (VEC) line producing GFP-tagged tPA, using total internal reflection-fluorescence (TIR-F) microscopy. tPA-GFP was detected in small granules in EA.hy926 cells, the distribution of which was indistinguishable from intrinsically expressed tPA. Its secretory dynamics were unique, with prolonged (> 5 minutes) retention of the tPA-GFP on the cell surface, appearing as fluorescent spots in two-thirds of the exocytosis events. The rapid disappearance (mostly by 250 ms) of a domain-deletion mutant of tPA-GFP possessing only the signal peptide and catalytic domain indicates that the amino-terminal heavy chain of tPA-GFP is essential for binding to the membrane surface. The addition of PAI-1 dose-dependently facilitated the dissociation of membrane-retained tPA and increased the amounts of tPA-PAI-1 high-molecular-weight complexes in the medium. Accordingly, suppression of PAI-1 synthesis in EA.hy926 cells by siRNA prolonged the dissociation of tPA-GFP, whereas a catalytically inactive mutant of tPA-GFP not forming complexes with PAI-1 remained on the membrane even after PAI-1 treatment. Our results provide new insights into the relationship between exocytosed, membrane-retained tPA and PAI-1, which would modulate cell surface–associated fibrinolytic potential. (Blood. 2009;113:470-478)

Introduction

Tissue plasminogen activator (tPA) is a 68-kDa serine protease that cleaves a single peptide bond in plasminogen to generate plasmin, which subsequently dissolves fibrin clots in the vasculature.[1] The expression of its activity is finely tuned by the amount of its specific inhibitor, plasminogen activator inhibitor-1 (PAI-1),[2,3] which is present in molar excess over tPA in human plasma. Thus, only a relatively small fraction of tPA circulates in blood in a functionally active form. Therefore, not only an elevation of plasma concentration of PAI-1 but an impairment of tPA release results in decreased fibrinolytic activity, which is regarded as a risk factor for ischemic cardiovascular events.[4-6] Although the enzymologic interactions of these 2 molecules in the fluid phase have been extensively studied, interactions at the interface between fluid-phase and solid-phase structures such as fibrin and the cell surface where functional fibrinolysis actually takes place are not fully elucidated.[7]

In blood, tPA is secreted primarily from vascular endothelial cells (VECs) as an active single-chain enzyme,[8] in contrast to most other serine proteases involved in coagulation and fibrinolysis, which are secreted as zymogens. Facilitated secretion, therefore, is directly related to the enhancement of fibrinolytic activity, which protects the VEC surface from clot accumulation and maintains vascular patency. Clinically, impairment of acute tPA release is reported in atherosclerosis, hypertension, and cigarette smoking.[9-12] VECs secrete tPA through both constitutive and regulated pathways[13-17] from small secretory granules morphologically distinct from the larger Weibel-Palade bodies.[18] Although the precise signaling pathways regulating tPA release have not been elucidated, G-protein–coupled activation and increased intracellular calcium signaling appear to be important.[15,17]

Recent advances in the use of fluorescent proteins, such as green fluorescent protein (GFP), have allowed us to visualize cellular events and cellular components in intact, living cells by monitoring fluorescence intensity and its localization within the cell. Several studies,[19-21] mainly in excitable cells, used GFP-tagged secretory molecules to document in detail the dynamics of their release from their granules, using total internal reflection-fluorescence (TIR-F) microscopy. This technique uses evanescent-wave excitation only of the fluorophore present in the immediate vicinity of the plasma membrane.

Using a similar approach, we conducted the present study to analyze the exocytotic dynamics of tPA in VECs under nonstimulated conditions. Slow secretory kinetics of tPA-GFP were demonstrated in VECs that exocytosed tPA-GFP molecules that are retained at the site on the cell membrane where the granules opened, and for which the amino-terminal heavy chain of tPA was required. Furthermore, PAI-1 appears to facilitate the dissociation of membrane-retained tPA, which would therefore decrease cell surface–associated fibrinolytic potential. These results provide new insights into the functional interactions of tPA and PAI-1 on the VEC surface.

Methods

Plasmid construction

The cDNA fragment encoding the enhanced green fluorescent protein (EGFP) from pEGFP-N1 (Clontech, Palo Alto, CA) was subcloned into *Nhe*I/*Not*I sites of the pcDNA3.1(+) expression vector and designated

Submitted March 7, 2008; accepted September 19, 2008. Prepublished online as *Blood* First Edition paper, October 15, 2008; DOI 10.1182/blood-2008-03-144279.

The online version of this article contains a data supplement.

The publication costs of this article were defrayed in part by page charge payment. Therefore, and solely to indicate this fact, this article is hereby marked "advertisement" in accordance with 18 USC section 1734.

GFP3.1. Total RNA from EA.hy926 cells was amplified by reverse-transcription–polymerase chain reaction (PCR) using the forward primer for the cDNA fragment encoding full-length human tPA excluding the stop codon (1686 bp) 5′-TT GCT AGC ATG GAT GCA ATG AAG AGA GGG-3′ and the reverse primer 5′-T TGG ATC CTT CGG TCG CAT GTT GTC ACG AAT-3′. The PCR product was digested with *Nhe*I and *Bam*HI and then subcloned into *Nhe*I/*Bam*HI sites in GFP3.1 (tPA-GFP). A mutant tPA containing a Ser-to-Ala substitution at amino acid position 478 (tPA-S478A-GFP) was produced using tPA-GFP as a template and a QuikChange II site-directed mutagenesis kit (Stratagene, La Jolla, CA). The forward and reverse primers were 5′-GCC TGC CAG GGC GAT GCG GGA GGC CCC CTG GTG-3′ and 5′-CAC CAG GGG GCC TCC CGC ATC GCC CTG GCA GGC-3′, respectively. A deletion mutant tPA-GFP (tPA-CD-GFP) was generated using a simple and rapid method by PCR.[22] A pair of primers, 5′-ACC TGC GGC CTG AGA CAG TAC-3′ and 5′-TTG GTA AGA TCT GGC TCC TCT-3′, was prepared for deleting tPA nucleotide positions 115 to 891 corresponding to amino acid position Val4-Ser262 (finger, epidermal growth factor-like, kringle 1, and kringle 2 domains; collectively FnEK1K2 domains, the so-called heavy chain).[23] All plasmid vectors were sequenced and prepared under endotoxin-free conditions.

Cell culture and transfection

The human vascular endothelial cell line EA.hy926 was kindly provided by Dr Edgell.[24] This cell line resembles cultured human VECs and has been shown to retain endothelial cell–specific functions in most respects, including their fibrinolytic characteristics.[25] We cultured the cells in Dulbecco modified Eagle medium (DMEM; Sigma-Aldrich, St Louis, MO) supplemented with glucose at 4.5 g/L and 10% fetal bovine serum at 37°C and 5% CO_2 in a humidified atmosphere. For fluorescence imaging, the cells were cultivated on a 35-mm glass bottom dish (Asahi Techno Glass, Tokyo, Japan) and transfected with the plasmids by lipofection using TransIT-LT1 (Mirus, Madison, WI) at 100% confluence. Experiments were performed within 2 days of transient transfection.

Suppression of PAI-1 synthesis

Cells were grown to 80% to 90% confluence in 35-mm glass bottom dishes and transfected with 20 nM siRNA for PAI-1 no. 1: 5′-GUC ACA UUG CCA UCA CUC UTT (Sigma-Aldrich), no. 4: 5′-AAG CAC AAC UCC CUU AAG GUC TT,[26] or siPerfect negative control (Sigma-Aldrich) using the N-TER Nanoparticle siRNA Transfection System (Sigma-Aldrich).

Solutions and materials

A HEPES-buffered solution (HBS) composed of 140 mM NaCl, 5 mM KCl, 1 mM $MgCl_2$, 2.5 mM $CaCl_2$, 10 mM glucose, and 10 mM HEPES-NaOH (pH 7.3) was used in all imaging studies unless otherwise noted. In some experiments, 50 mM NaCl was replaced by 50 mM NH_4Cl. Low-pH solution (pH 5.5) was buffered with Mes in place of HEPES. Human recombinant PAI-1 was purified as previously described.[27] Human recombinant single-chain tPA (sc-tPA) was kindly provided by Daiich Seiyaku (Tokyo, Japan). Human Glu-plasminogen was purified from freshly frozen human plasma by affinity chromatography on lysine-Sepharose. Human thrombin was from Benesis (Osaka, Japan). Human fibrinogen and receptor-associated protein (RAP) were purchased from Enzyme Research Laboratories (South Bend, IN) and Calbiochem (Darmstadt, Germany), respectively. Anti-GFP and anti-GFP conjugated with tetramethylrhodamine isothiocyanate (TRITC) were from Molecular Probes (Eugene, OR) and Acris Antibodies (Hiddenhausen, Germany), respectively. Anti-tPA and anti–PAI-1 were produced in rabbits using human recombinant sc-tPA or PAI-1; the IgG fractions were isolated from the antiserum.

Imaging experiments

We used a TIR-F microscopy unit for selective excitation only near the plasma membrane[28,29] and its associated granules. Cells were imaged with an inverted microscope (IX71; Olympus, Tokyo, Japan) equipped with a 60×/1.45 numeric aperture (NA) oil-immersion objective (for TIRFM; Olympus) to generate the so-called "evanescent field." The evanescent wave selectively excites fluorophores within 100 nm of the glass-water interface. To reduce the bleaching of fluorophores and laser-derived cell damage, we introduced neutral density filters (Edmund Optics, Tokyo, Japan) to reduce laser intensity to 12.5%. Bleaching of intracellular fluorophore was then suppressed to less than 10% using ND filters. GFP was excited at 488 nm, and the emitted light was collected. In some experiments, both GFP and TRITC were excited at 488 nm, and the light emitted was collected through an emission splitter (W-View system; Hamamatsu Photonics, Hamamatsu, Japan) equipped with a 550-nm dichroic mirror and 2 emission filters, a 510/23-nm bandpass filter for GFP and 600-nm long-pass filter for TRITC. The fluorescence images were captured and recorded simultaneously through a cooled (− 50°C) charge-coupled device (CCD) digital camera (ORCA-ER; Hamamatsu Photonics) or high-sensitivity electron multiplier CCD (EM-CCD; ImagEM; Hamamatsu Photonics) camera controlled by AQUACOSMOS Imaging Station (Hamamatsu Photonics). We measured the fluorescence intensity of the GFP or TRITC in single granules. These values (F) were normalized to their initial values, F_0 (ie, when the granules had docked but were still unopened) and the relative fluorescence change is referred to as F/F_0.

Cells transiently expressing GFP-tagged proteins were washed 3 times with HBS and incubated with fresh HBS for signal recording. Cells were kept at 37°C on the microscope stage (INUG2-ONID-BE; Tokai Hit, Shizuoka, Japan). In some experiments, a gravity-fed perfusion system was used to exchange HBS for NH_4Cl solution, Mes-buffered pH 5.5 solution. The solutions were warmed at 37°C by an in-line heater with automatic temperature controller (Warner Instruments, Hamden, CT).

Immunocytochemistry

tPA-GFP–expressing or nonexpressing EA.hy926 cells cultured on a coverslip were fixed with 4% paraformaldehyde in PBS for 30 minutes and permeabilized by 0.1% Triton X-100 for 15 minutes. After blocking with 2% bovine serum albumin, cells were stained with 5 μg/mL anti-tPA for 1 hour, followed by Alexa Fluor 488– or TRITC-conjugated anti-IgG immunoglobulin (Molecular Probes and Dako, Carpinteria, CA) for 1 hour. After being mounted on a glass microscope slide with Dako fluorescent mounting medium, the specimens were examined by both epifluorescence (epi-F) and TIR-F microscopy.

Western blotting and fibrin autography

Culture medium was collected after 1 or 24 hours and centrifuged at 3000*g* for 10 minutes to remove cell debris. It was then mixed with the sample buffer for SDS–polyacrylamide gel electrophoresis (PAGE). After separation by SDS-PAGE, protein bands were trans-blotted onto a nitrocellulose membrane. tPA-, PAI-1–, and GFP-related bands were then visualized by anti-tPA, anti–PAI-1, or anti-GFP antibody, respectively, followed by horseradish peroxidase (HRP)–conjugated secondary antibodies, using enhanced chemiluminescence (ECL) Western blotting detector reagents (GE Healthcare, Little Chalfont, United Kingdom). For fibrin autography, protein bands in the culture medium were similarly separated by SDS-PAGE, and tPA-dependent activity was detected by plasminogen-rich fibrin indicator gels as described previously.[30]

Results

tPA-GFP localizes in the secretory granules and is secreted into the medium in a functional form from VECs (EA.hy926 cells)

We first characterized tPA-GFP expressed in EA.hy926 cells. Its intracellular localization was visualized by both epi-F and TIR-F microscopy, and was compared with intrinsically expressed tPA in EA.hy926 cells. The latter was detected by anti-tPA antibody labeled with FITC in small, round secretory granules (Figure 1A) as reported by Emeis et al in human umbilical vein endothelial cells

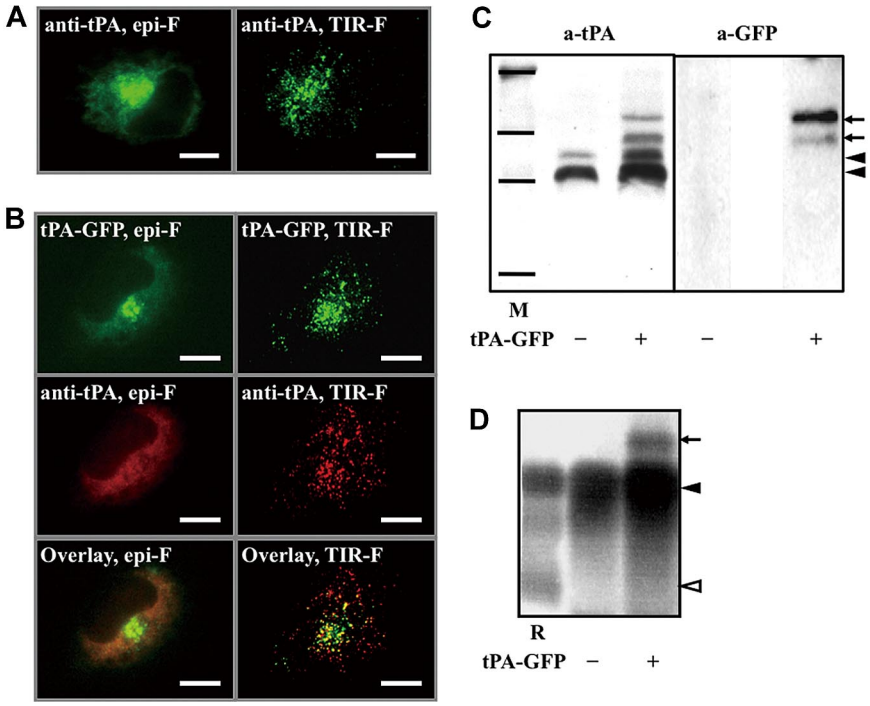

Figure 1. Properties of tPA-GFP expressed in EA.hy926 cells. Intracellular localization of intrinsic tPA (A) and forcibly expressed tPA-GFP (B) in confluent EA.hy926 cells analyzed by immunofluorescence staining and represented by both epifluorescence (epi-F) and total internal reflection-fluorescence (TIR-F) images. (A) Intrinsically expressed tPA molecules in EA.hy926 cells detected by anti-tPA antibody together with Alexa Fluor 488–labeled anti-IgG. (B) tPA-GFP (top panels) and tPA-related proteins detected by anti-tPA antibody together with TRITC-labeled anti-IgG (middle panels). The bottom panels are the merged images of the top and middle panels. The bars represent 10 μm. (C) Western blotting of 24-hour culture media from untransfected cells or transfected with tPA-GFP expression vector. Protein bands were detected by either anti-tPA or anti-GFP antibody. (D) The same samples in panel C were also analyzed by plasminogen-rich fibrin autography. M indicates molecular weight markers for 201, 120, 100, and 56 kD; R, a mixture of recombinant tPA and recombinant PAI-1; ◀, tPA-PAI-1 complexes; and ◁, free tPA. Extra-high-molecular-weight bands in culture medium from tPA-GFP–expressing cells (↤) were detected by both anti-tPA and anti-GFP antibodies, and developed lytic bands in fibrin autography.

(HUVECs).[18] tPA-GFP fluorescence was detected in similar small granules in EA.hy926 cells. It was also detected by anti-tPA antibody labeled with TRITC, and its distribution in EA.hy926 cells was indistinguishable from intrinsically expressed tPA, which was more clearly and distinctly visualized by TIR-F (Figure 1B).

We next characterized tPA-GFP enzymatic activity at 24 hours in culture medium from either nontransfected EA.hy926 cells or those transfected with tPA-GFP expression vector. Western blot analysis (Figure 1C) using anti-tPA antibody revealed a high-molecular-weight band, approximately 147 kDa, in culture medium from the tPA-GFP–expressing cells that was absent from controls. This band was also detected by anti-GFP antibody, suggesting that it corresponded to a tPA-GFP-PAI-1 complex. Bands corresponding to both free tPA-GFP and intrinsic tPA were not observed because of the high level of expression of PAI-1 in this cell line. The high-molecular-weight band was also visualized by fibrin zymography (Figure 1D), suggesting that tPA-GFP is enzymatically active, forming high-molecular-weight complexes with PAI-1 and developing lytic bands in plasminogen-rich fibrin gels. These results suggest that tPA-GFP was secreted in an active form into the supernatant from the granules that contained it, in the same way as the intrinsic tPA. Therefore, tPA-GFP appeared to be functional and thus to represent a suitable probe for investigating the secretory mechanism of tPA in VECs.

Sequential steps (recruitment, docking, opening, and release) of tPA-GFP secretory granular exocytosis are visualized by TIR-F microscopy

To investigate processes by which tPA-GFP was released from its secretory granules, we performed time-lapse analysis using TIR-F microscopy. This has the advantage that molecular events taking place near the plasma membrane can be analyzed, and has been applied mainly to excitable cells.[19-21] TIR-F illuminates to a depth of 100 nm or lower from the glass coverslip into the specimen because the energy wave drops off exponentially with distance from the coverslip-specimen interface. Using this technique, several sequential steps leading to single granular exocytosis of tPA-GFP were visualized as changes of fluorescence intensities. First, the recruitment of tPA-GFP–containing granules to the evanescent field and subsequent docking to the plasma membrane were imaged as the appearance of a static fluorescent spot. Second, granular opening was recognized as a sudden increase in fluorescence due mainly to neutralization of acidic pH in tPA-GFP–containing granules by culture medium at neutral pH. Indeed, a spatial shift of tPA-GFP closer to the coverslip during granule opening also contributes to the increase in fluorescence. To confirm that the sudden increase in fluorescence does indeed represent the opening of tPA-GFP–containing granules, we analyzed simultaneous temporal profiles of fluorescence intensities of tPA-GFP and TRITC-conjugated anti-GFP antibody. Figure 2A shows that a sudden increase (arrowhead) in green fluorescence of tPA-GFP corresponded to a gradual increase in red fluorescence, indicating that TRITC-conjugated anti-GFP antibody present in the extracellular space accumulated in the single opened granular spot. Every opened granule showed this gradual accumulation of red fluorescence (72 granules from 9 cells in 5 independent experiments). Evidently, sudden brightening of the secretory granule containing fluorescent tPA signifies the connection of the interior of the granule with the extracellular space. Third, the release of the contents of the granules was recognized by a decrease in fluorescence intensity. Because this third step is itself composed of several distinct steps, it will be described in detail later. Thus, we defined these 3 sequential main stages of change in fluorescence intensity as reflecting the secretory process.

The third stage of the tPA-GFP secretory process (ie, cargo release into the extracellular space according to this definition) was more heterogeneous than the other 2 steps. To evaluate this, we attempted to estimate the kinetics of tPA-GFP release from opened granules. We calculated the time required for the fluorescence intensity to decline to half of its peak value during the exponential reduction period following the sudden brightening due to granule opening, which we designated $T_{F1/2}$. The individual $T_{F1/2}$ during the

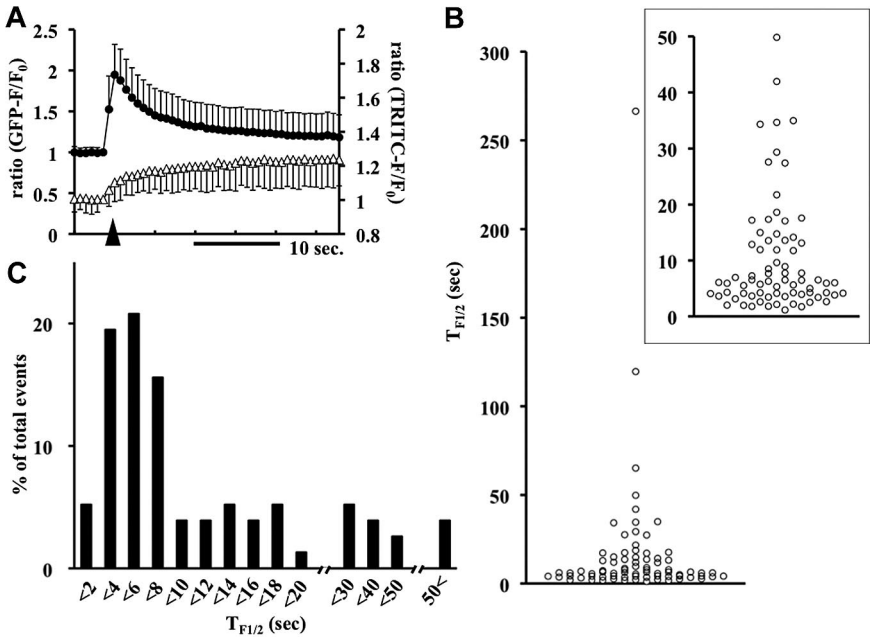

Figure 2. Secretory kinetics of tPA-GFP determined by TIR-F microscopy. (A) Secretory kinetics of tPA-GFP in EA.hy926 cells analyzed by TIR-F microscopy using recording medium containing 50 μg/mL TRITC-conjugated anti-GFP antibody. Changes in the fluorescence intensities of both GFP and TRITC were monitored simultaneously through W-View system at 1.4 Hz. The means plus or minus SD of relative changes in fluorescence intensity (F/F_0) of tPA-GFP (●) and TRITC-conjugated anti-GFP antibody (△) in 72 granules from 9 cells tested are shown in panel A (5 independent experiments). Sudden increase in green fluorescence (▲) was followed by a gradual increase in red fluorescence. (B) Individual $T_{F1/2}$ (the time required for the fluorescence to decline to half of its peak value), which defines the half-life of exocytosed tPA-GFP disappearance from the membrane surface, are plotted (77 granules in 10 cells). Expanded time points within 50-second $T_{F1/2}$ are shown in the inset. (C) Number of total occurrences calculated for individual $T_{F1/2}$ (abscissa) shown as percentages of total occurrences (ordinate).

tPA-GFP–releasing process varied widely from a maximum of 266 seconds to a minimum of 1.13 seconds. This was analyzed and plotted for 77 granules in 10 cells (Figure 2B,C). Notably, almost all the fluorescent spots of exocytosed tPA-GFP, even those with the shortest $T_{F1/2}$, remained detectable during the entire recording period (4.7 minutes). Similar heterogeneity in the dynamics of fluorescent protein–labeled tPA release has also been described previously in bovine chromaffin cells[31] and in insulin-producing MIN6 cells.[32] However, the underlying mechanisms and reasons for this have not yet been determined.

tPA-GFP is retained on the membrane surface in a VEC-specific manner

The slow dimming of tPA-GFP fluorescence after granule opening was further analyzed. Several factors may contribute to this process: (1) diffusion of tPA-GFP from the site of the opened granule into the liquid phase; (2) diffusion of tPA-GFP into the plasma membrane but retention at the membrane surface (lateral diffusion); and (3) recapturing (granule resealing) and reacidification of tPA-GFP–containing granules. We first analyzed the last possibility and asked whether the postexocytotic spots of tPA-GFP are retained on the membrane surface. Taking advantage of GFP fluorescence quenching on acidification, we analyzed the effect of transiently exposing tPA-GFP–expressing EA.hy926 cells to Mes-buffered acidic pH solution (pH 5.5 solution, applied 3 times for 30 seconds every 5 minutes). The degree of fluorescence of a granule that had brightened once on opening (Figure 3A arrowhead) and was then in the process of dimming further decreased at pH 5.5 and was reversed on neutralization. This reversible dimming, detected as a relative fluorescence decrease more than 20%

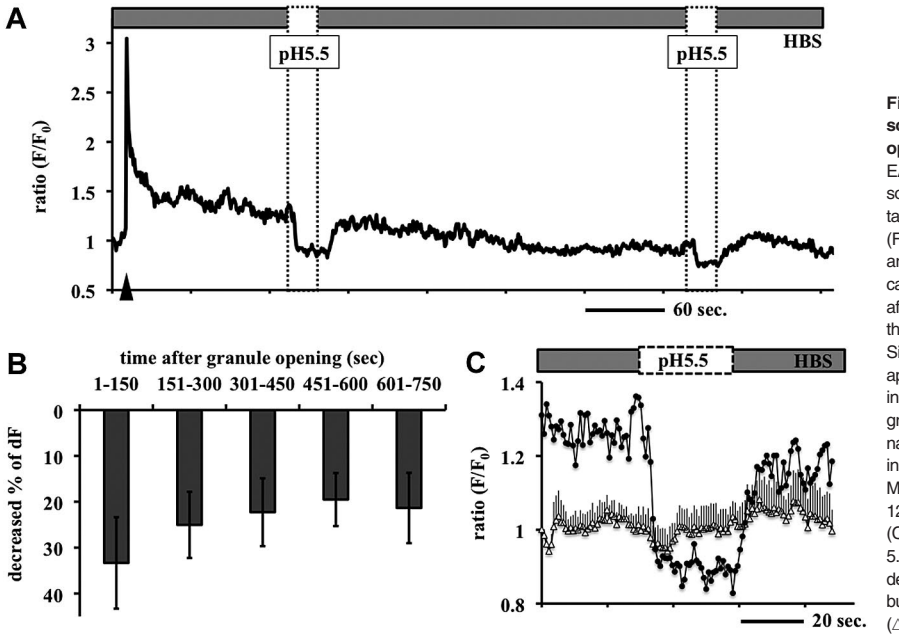

Figure 3. Effects of perfusion of Mes-buffered pH 5.5 solution on the fluorescence intensity of tPA-GFP after opening of the granules. (A) tPA-GFP–expressing EA.hy926 cells were perfused with Mes-buffered pH 5.5 solution for 30 seconds every 5 minutes, 3 times. Representative data on the relative changes in fluorescence intensity (F/F_0) of tPA-GFP in one single secretory granule at 1.4 Hz are shown. Application of pH 5.5 solution (dashed box) caused an abrupt decrease in GFP fluorescence intensities after exocytosis, which was quickly recovered on neutralizing the pH (HBS). Arrowhead indicates opening of the granule. Similar fluctuations were observed even at the second application of the pH 5.5 solution in 45 (67%) of 67 granules in 5 independent experiments. (B) Abscissa: time after granule opening before application of pH 5.5 solution; ordinate: percentage decrease in relative fluorescence intensity in individual granules after application of pH 5.5 solution. Mean plus or minus SD in each time category from 126 events of pH 5.5 application in 67 opened granules. (C) Expanded graph of panel A at the first application of pH 5.5 solution. Application of pH 5.5 solution triggered the decrement of GFP fluorescence in postexocytotic spots (●), but did not significantly change this in unopened granules (△, mean ± SE from 6 granules).

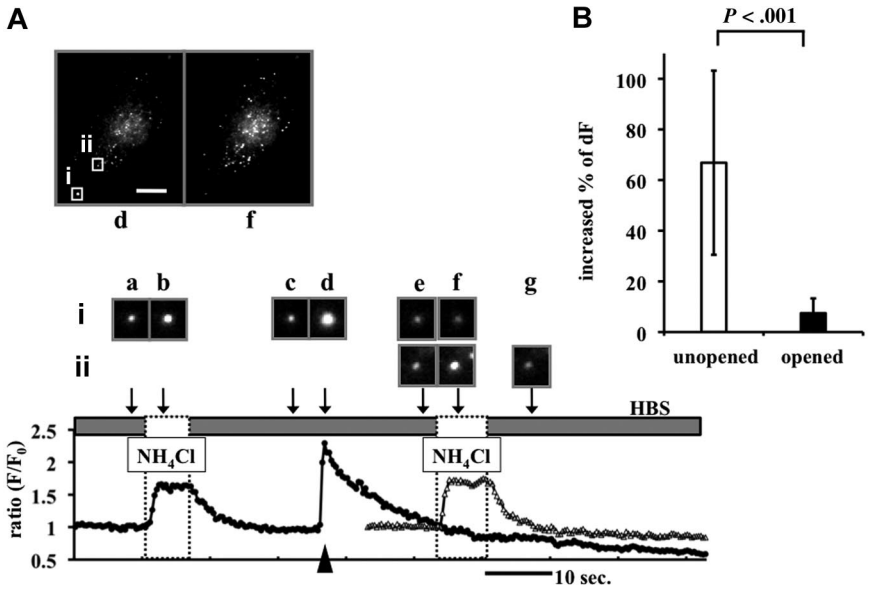

Figure 4. Effects of perfusion of NH_4Cl solution on the fluorescence intensity of tPA-GFP before and after opening of the granules. (A) tPA-GFP–expressing cells exposed to 50 mM NH_4Cl solution (dashed box). Representative data on F/F_0 of tPA-GFP secretory granules opened (filled circles, granule i, opened at time "d") and not opened (open triangles, granule ii) at 1.4 Hz. Top panels: images of whole cell at point d (opening, arrowhead) and f (NH_4Cl exposure). The bar represents 10 μm. Middle panels (a-g): images taken at the times indicated by the arrows from opened (i) and unopened (ii) granules. Brief application of NH_4Cl increased fluorescence intensity of tPA-GFP in unopened granules (i at time "b," ii at time "f"), but not opened granules (i at time "f"). (B) Percentage increase in relative fluorescence intensity from 111 unopened and 43 opened tPA-GFP–containing granules in 6 cells on NH_4Cl exposure. Five independent experiments are shown as mean plus or minus SD. In the analysis of opened granules, the mean time after granule opening to NH_4Cl exposure was 5.85 minutes.

(Figure 3B), persisted for as long as the fluorescent spots were detectable (tested on 67 granules in 6 cells; 5 independent experiments). This was longer than 5 minutes in 45 (67%) of these 67 granules. In contrast, we also traced unopened granules at this time (albeit very few of them because of their motility) and found that their relative changes of fluorescence intensity were not influenced by expose to pH 5.5 (Figure 3C open triangles). These results indicate that the exocytosed tPA-GFP retained on the membrane surface during this observation period and that material is not recaptured. Further, we applied NH_4Cl as a source of NH_3 to tPA-GFP–expressing EA.hy926 cells. This penetrates the plasma membrane and neutralizes the acidic pH in intracellular organelles. Transient exposure to NH_4Cl resulted in a 66.8% plus or minus 36.3% increase in fluorescence intensity of tPA-GFP (Figure 4B) before the secretory granule opened (Figure 4A point b). Once the granule had opened, however, none of the 43 granules tested in 6 cells showed any significant increase in fluorescence intensity on NH_4Cl exposure (Figure 4A point f, Figure 4B). This is in contrast to tPA-GFP expressed in insulin-producing MIN6 cells in which almost all the opened granules seemed to have been recaptured and reacidified. When tPA-GFP–expressing MIN6 cells were depolarized by 40 mM potassium followed by NH_4Cl 60 to 90 seconds later, the fluorescence intensity of 13 of 14 opened granules as well as 258 unopened granules from 4 cells was increased (data not shown). These results indicate that the exocytosed tPA-GFP was retained at the membrane surface without retrieval for more than 5 minutes in a VEC-specific manner. The dimming of tPA-GFP fluorescence after granule opening appeared to result mainly from diffusion of tPA-GFP from the site of the opened granule membrane into the fluid phase and/or plasma membrane nearby in VECs.

FnEK1K2 domains are responsible for binding of tPA-GFP to the membrane surface

To investigate the mechanism of the slow release of tPA-GFP after exocytosis, we constructed a mutant tPA lacking the heavy chain and possessing only the signal peptides and catalytic domain and fused this with GFP (tPA-CD-GFP). The heavy chain of tPA is composed of finger, epidermal growth factor-like, kringle1, and kringle2 (FnEK1K2) domains (Figure 5A), and especially Fn and K2 domains play an important role in binding to fibrin clots.[23] The intracellular distribution of tPA-CD-GFP was similar to wild-type tPA-GFP in both epi-F and TIR-F microscopy imaging (Figure 5B). In wild-type, the reduction in fluorescence after rapid brightening in opened single secretory granules was slow (Video S1 [available on the *Blood* website; see the Supplemental Materials link at the top of the online article]: tPA-GFP at 1 Hz). In contrast, tPA-CD-GFP fluorescence disappeared immediately after opening, like a flashlight being turned off, and did not leave any fluorescent spots of postexocytotic tPA-CD-GFP (Video S2: tPA-CD-GFP at 1.4 Hz). When NH_4Cl solution was transiently applied to tPA-CD-GFP–expressing cells, all granule spots in the TIR-F area increased in brightness (270 granules in 6 cells), suggesting that tPA-CD-GFP molecules were not retained on the membrane surface but were present only in unopened granules. These results indicate that tPA-CD-GFP could not be retained on the membrane surface because of the lack of the FnEK1K2 domain. The reduction in fluorescence after opening in domain-deletion mutants of either Fn or K2 of tPA-GFP–expressing cells was also faster than that in wild-type (Figure S1), suggesting the importance of these domains in the binding.

To evaluate the rapid discharge of tPA-CD-GFP, we acquired images with a highly sensitive electron multiplier CCD (EM-CCD) camera to improve time resolution. Figure 5C shows the 32 frames per second (fps) sequences of tPA-CD-GFP discharge from a single granule. After granule opening shown at time 0 ms, fluorescence diffused and had mostly disappeared by 250 ms. In this short period of time, in contrast, the fluorescence of exocytosed wild-type tPA-GFP remained strong (Figure 5D). The rapid time course of disappearance of tPA-CD-GFP was similar to the exocytotic time course of neuropeptide Y (NPY)–GFP in PC12 cells.[33] Therefore, FnEK1K2 domains appeared responsible for the binding of exocytosed tPA-GFP to the membrane surface as well as for the heterogeneous dynamics of the tPA release process.

PAI-1 accelerates membrane surface–retained tPA dissociation

Because tPA-GFP as well as intrinsic tPA were observed only as a complex with PAI-1, and essentially no free form was detected in the supernatant, we investigated the effects of PAI-1 on the

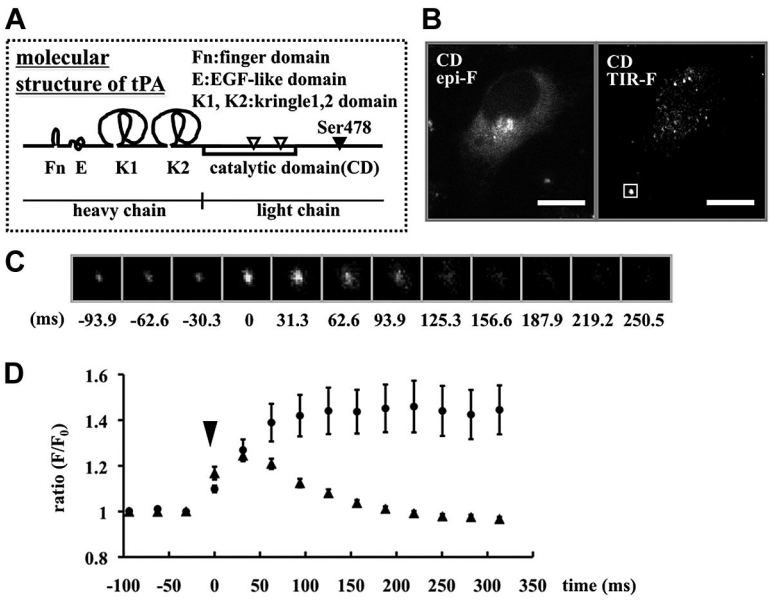

Figure 5. High time-resolution analysis of the secretory dynamics of tPA-CD-GFP. (A) Molecular structure of tPA. (B) Epi-F and TIR-F images in tPA-CD-GFP–expressing cells. The bars represent 10 μm. (C) Representative 32 frames per second sequences of the single tPA-CD-GFP secretory granule indicated by a white box in panel B. Time 0 shows the point of granule opening. (D) Changes in F/F_0 in each single secretory granule plotted as a function of the time after opening (time 0) of tPA-CD-GFP–containing granules (▲, 31 granules from 6 cells) compared with tPA-GFP–containing granules (●, 8 granules from 3 cells). Data are shown as mean plus or minus SE.

dynamics of tPA release using 3 different approaches: (1) supplementation with recombinant PAI-1, (2) use of a GFP-tagged mutant form of tPA, tPA-S478A-GFP, and (3) suppression of PAI-1 synthesis by siRNA. In the first approach, we analyzed the effect of recombinant PAI-1 (rPAI-1) in tPA-GFP–expressing EA.hy926 cells. $T_{F1/2}$ values before and after the addition of 40 nM rPAI-1 were calculated. Although the frequency of granule opening during each of the 4.7-minute observation periods was similar (53 granules before addition and 55 granules after addition opened in 6 cells; 4 independent experiments), $T_{F1/2}$ was significantly reduced on addition of 40 nM rPAI-1 (Figure 6A). This accelerated reduction in fluorescence intensity in postexocytotic spots after rPAI-1 treatment was also detected even after pretreatment with 400 nM receptor-associated protein (RAP), which antagonizes the binding of tPA and tPA-PAI-1 complex to the low-density lipoprotein receptor-related protein (LRP; Figure 6C). When the cells were incubated with rPAI-1 for 60 minutes, tPA increased in a dose-dependent manner in the supernatant only in the form of a complex with rPAI-1, as detected by fibrin autography (Figure 6B). PAI-1 appeared to facilitate the dissociation not only of tPA-GFP but also intrinsic tPA from the granule membrane surface by forming high-molecular-weight complexes. In the second approach, we constructed a GFP-tagged mutant form of tPA, tPA-S478A, in which Ser478 was substituted by Ala so as to be catalytically inactive and unable to form covalent complexes with PAI-1, and analyzed its exocytotic dynamics. Although the efficacy of expression of tPA-S478A-GFP and wild-type tPA-GFP was similar, the former did not appear in the culture medium after 24 hours either complexed with PAI-1 or in the free form (Figure 7A). The intracellular distribution of tPA-S478A-GFP and tPA-GFP was indistinguishable, as judged by epi-F. In contrast, however, TIR-F revealed much stronger fluorescence of tPA-S478A-GFP than wild type (Figure 7B), suggesting that it is present at higher concentrations near the plasma membrane. The secretory dynamics of tPA-S478A-GFP also differ from wild type (Video S3), and it remained attached to the membrane surface for a longer period of time after granules' opening. Eventually it did diffuse away into the plasma membrane, because strong fluorescence was observed not only in secretory granular spots but also in the surrounding plasma membrane. The presence of large amounts of tPA-S478A-GFP on the exterior plasma membrane was further confirmed by the fact that the decreasing intensity of fluorescence in whole cells measured by epi-F image (dF_{cell}) was more pronounced for tPA-S478A-GFP than wild type when cells were exposed to pH 5.5 solution (Figure 7C). Lack of formation of high-molecular-weight complexes between tPA-S478A-GFP and PAI-1 seems to render detachment from the membrane surface difficult, which eventually resulted in its accumulation on the cell surface. Accordingly, exogenous PAI-1 did not affect the prolonged $T_{F1/2}$ in single granules containing tPA-S478A-GFP (Figure 7D gray bars). In the third approach, to more clearly demonstrate the effect of exogenous rPAI-1 on membrane surface–retained tPA, EA.hy926 cells were treated with PAI-1 siRNA to negate the effects of intrinsically synthesized PAI-1. Transient transfection with 2 different sequences (nos. 1, 4) of 20 nM PAI-1 siRNA reduced the amount of free PAI-1 in the culture medium after 18 hours, although complexes with tPA did not change a great deal (Figure 7E). Under such conditions, $T_{F1/2}$ was prolonged significantly in comparison with control siRNA–transfected cells (no. 1: 23.9 ± 3.56 seconds from 141 granules, no. 4: 23.0 ± 4.80 seconds from 40 granules vs control siRNA: 8.1 ± 0.47 seconds from 113 granules; $P < .001$; data given as means ± SE) (Figure 7F). These effects of PAI-1 siRNA were prevented by the addition of 40 nM rPAI-1 (Figure 7G), reverting to the values for nontreated EA.hy926 cells as shown in Figure 6A. PAI-1, therefore, appeared to regulate the amounts of cell surface–associated tPA on VECs by facilitating the dissociation of tPA from the cell surface.

Discussion

Here, we demonstrated unique, slow secretory dynamics of tPA in VECs. In EA.hy926 cells, tPA-GFP was retained as fluorescent spots on the membrane surface after secretory granule opening without any internalization for more than 5 minutes. This contrasts with the exocytotic dynamics of tPA-containing secretory granules in endocrine and neuronal cells where postexocytotic tPA granules are retrieved, as described by "kiss-and-run" or "cavicapture" models.[21,31-34] In the present study, we showed for the first time that the FnEK1K2 domains in tPA molecule are responsible for the

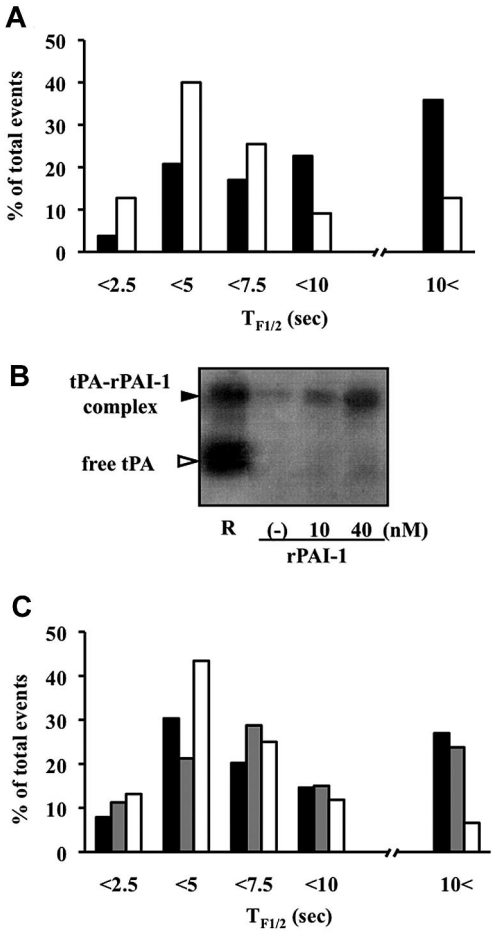

Figure 6. The effect of recombinant PAI-1 on membrane surface–retained tPA. (A) $T_{F1/2}$ values of tPA-GFP (abscissa) before (■: 53 granules) and after (□: 55 granules) addition of 40 nM recombinant PAI-1 (6 cells, 4 independent experiments) shown as percentages of total occurrences (ordinate). Exogenous PAI-1 increased the frequency of rapidly disappearing fluorescence having short $T_{F1/2}$. (B) Fibrin autography of the supernatants of the cells incubated with exogenous rPAI-1 at 0, 10, and 40 nM for 60 minutes. The amounts of tPA increased as a function of the amounts of added PAI-1, in the form of a tPA-PAI-1 complex in the supernatant. A representative image from 5 independent experiments is shown. (C) $T_{F1/2}$ values of tPA-GFP (abscissa) before (■: 89 granules), after incubation with 400 nM RAP (▩: 80 granules), and after further addition of 40 nM recombinant PAI-1 (□, 76 granules) from 6 independent experiments shown as percentages of total occurrences (ordinate). The presence of RAP did not change the effect of PAI-1 as shown in panel A.

retention of exocytosed tPA on the cell surface. Retention of the active form of tPA on the cell surface without retrieval may be beneficial for maintaining high fibrinolytic activity. Further, using 3 different approaches, we demonstrated that PAI-1, the primary inhibitor of tPA, facilitates tPA dissociation from the VEC surface and functions as principal determinant of fibrinolytic activity on VECs as well as in plasma.

A unique characteristic of the tPA-releasing process in VECs is the extended period during which exocytosed tPA is retained on the surface of the cell without either retrieval or internalization. This was confirmed by 2 distinct experiments. One is the quenching of fluorescence of tPA-GFP spots by transient application of pH 5.5 solution to tPA-GFP–expressing EA.hy926 cells. The quenching was observed only in the spots that had already opened and persisted for as long as the fluorescent spots were detected. Another finding, that RAP did not modify the kinetics of the disappearance of tPA-GFP from the membrane, may suggest that the internalization of tPA or tPA-PAI-1 through LRP is not the major mechanism mediating tPA disappearance from the membrane surface.

In VECs, exocytosis mechanisms have been intensively studied[35-37] in other large rod-shaped regulated secretory granules, known as Weibel-Palade bodies (WPBs). WPBs contain von Willebrand factor (VWF), endothelin, interleukin-8, and several adhesion molecules such as P-selectin and CD63. Romani de Wit et al assessed the trafficking of WPBs during signal-mediated exocytosis in living VWF-GFP–infected HUVECs and showed that the granules were retained as extracellular patches after opening evoked by both Ca^{2+} and cAMP-mobilizing agonists.[38] Similarly to our present results on tPA-GFP–containing granules, individual VWF-GFP patches remained visible for approximately 20 minutes.[39] Although the precise mechanisms responsible for these phenomena have not been clarified yet, such sustained retention of cargos after exocytosis appears common to both tPA and VWF in VECs.

When a mutant tPA-GFP lacking FnEK1K2 domains (tPA-CD-GFP) was used, the fluorescence disappeared in as short as 250 ms without leaving any fluorescent spots. This confirms that FnEK1K2 domains are responsible for the retention of tPA molecules on the membrane. tPA is known to bind to fibrin and denatured proteins having cross beta structures,[40] and to efficiently catalyze plasminogen activation in which finger and K2 domains are reported to be responsible.[41] The K2 domain possesses so-called lysine-binding sites (LBSs), and binds to proteins bearing C-terminal lysine either on cell membranes or in plasma. It now appears that FnEK1K2 domains, especially finger and K2 domains, are also responsible for the retention of postexocytotic tPA molecules on the cell surface.

Although the FnEK1K2 domains of the tPA molecule are responsible for its retention on the membrane surface, no plasma membrane–associated tPA-binding factor has been identified in the present study. Among several proteins known to bind to tPA,[42] annexin A2 is a particularly good candidate because it binds both tPA and plasminogen, and thereby facilitates plasmin generation on the endothelial cell surface.[43,44] In most previous studies, however, direct interactions between annexin A2 and intrinsically generated and exocytosed tPA were not investigated. We analyzed possible binding of exocytosed tPA-GFP to annexin A2 on the surface of EA.hy926 cells. However, we failed to demonstrate colocalization of tPA-GFP with intrinsically generated annexin A2 either by immunocytochemistry or by using monomeric red fluorescent protein (mRFP)–tagged annexin A2 in EA.hy926 cells (data not shown). We hypothesize, therefore, that de novo synthesized tPA is present in the secretory granules and/or membrane surface bound via FnEK1K2 domains to unidentified factors other than annexin A2 even after exocytosis. Another possibility that exocytosed tPA binds to the matrix in the localized area is also not excluded, and further study is needed to identify the binding factor for tPA.

This sustained retention of tPA may be beneficial for maintaining functional fibrinolytic activity, because the secreted single-chain tPA is enzymatically active[8] and the VEC surface is the site where fibrinolytic components assemble and mediate their functions.[7] We successfully demonstrated the cell surface–retained intrinsic tPA activity after suppression of PAI-1 synthesis by siRNA transfection in EA.hy926 cells, which was totally inhibited by supplemented rPAI-1 (Figure S2). PAI-1 seems to suppress tPA activity not only in the fluid phase but also in solid-phase structures, on the cell surface, by facilitating the dissociation of membrane-retained intrinsic tPA. The facilitated dissociation of tPA-GFP by supplemental rPAI-1 was more clearly shown when intrinsic PAI-1 synthesis was suppressed by siRNA, suggesting that

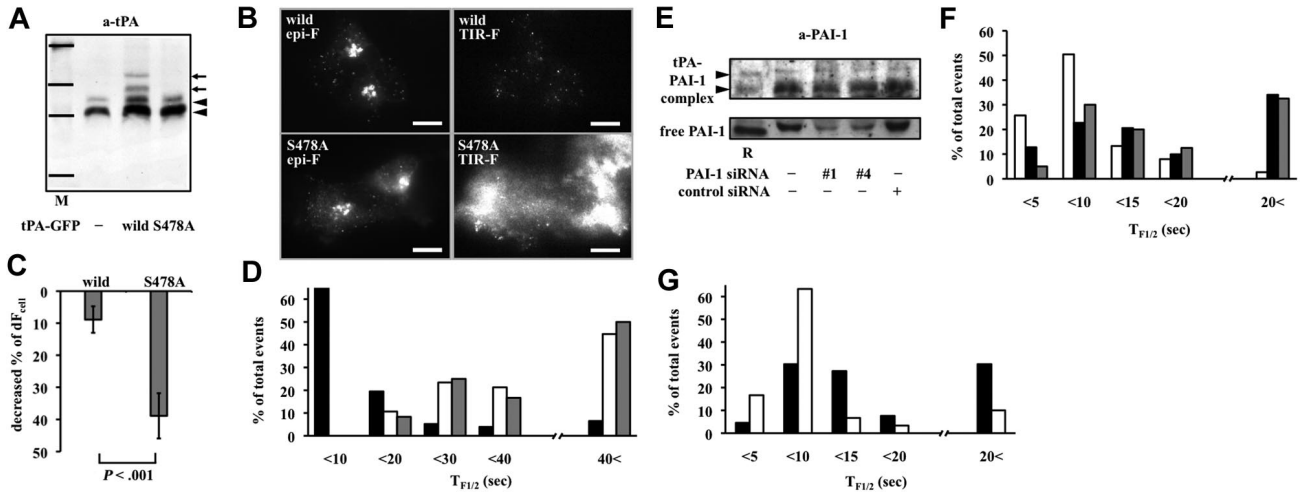

Figure 7. Secretory dynamics of tPA-S478A-GFP and tPA-GFP in PAI-1 siRNA–transfected cells. (A) Twenty-four–hour culture media from tPA-GFP–expressing (wild type) or tPA-S478A-GFP–expressing (S478A) cells analyzed by Western blotting using anti-tPA antibody. M indicates molecular weight markers for 201, 120, 100, and 56 kDa; ◀, tPA-PAI-1 complex. Additional high-molecular-weight bands of tPA-GFP-PAI-1 complexes (↼), which reacted with anti-tPA antibody, were detected only in culture media from tPA-GFP–expressing cells. (B) Epi-F and TIR-F images in tPA-GFP– and tPA-S478A-GFP–expressing cells. tPA-S478A-GFP appeared diffusely distributed over the membrane surface as shown in the TIR-F image. The bars represent 10 μm. (C) Cells expressing either tPA-GFP (wild type, 11 cells) or tPA-S478A-GFP (S478A, 13 cells) were exposed to Mes-buffered pH 5.5 solution for 1 minute, and the decrease in relative fluorescence intensity in a whole cell was measured by epi-F image (dF_{cell}) calculated. Decrease in fluorescence intensity was significantly greater in tPA-S478A-GFP cells than tPA-GFP cells. Data are shown as mean plus or minus SD. (D) $T_{F1/2}$ values (abscissa) in tPA-GFP (■, 77 granules in 10 cells), tPA-S478A-GFP (□, 54 granules in 7 cells), and tPA-S478A-GFP supplemented with 40 nM rPAI-1 (▩, 12 granules in 2 cells) shown as percentages of total occurrences (ordinate). Exogenous PAI-1 did not modify the slow disappearance, having long $T_{F1/2}$ in tPA-S478A-GFP–expressing cells. (E) Eighteen-hour culture media from siRNA (PAI-1 no. 1, no. 4, and control)–transfected cells analyzed by Western blotting using anti–PAI-1 antibody. R indicates mixture of recombinant tPA-PAI-1 complexes and free PAI-1. (F) $T_{F1/2}$ values (abscissa) of tPA-GFP in control siRNA–treated (□, 113 granules in 8 cells, 5 experiments), PAI-1 siRNA no. 1–treated (■, 141 granules in 10 cells, 5 experiments), and PAI-1 siRNA no. 4–treated (▩, 40 granules in 3 cells, 3 experiments) cells, shown as percentages of total occurrences (ordinate). (G) $T_{F1/2}$ values (abscissa) of tPA-GFP before (■, 66 granules) and after (□, 30 granules) addition of 40 nM rPAI-1 in PAI-1 siRNA no. 1 or no. 4 transfected cells (3 experiments) shown as percentages of total occurrences (ordinate). Exogenous PAI-1 increased the frequency of rapid disappearing granules having short $T_{F1/2}$.

disappearance of tPA-GFP, which was slow as shown in the present study, was still under the control of intrinsically generated PAI-1 in EA.hy926 cells. Another finding, that tPA-S478A-GFP stayed on the cell membrane for a long period, suggests that PAI-1 is the principle modifier of both the duration and amount of tPA retained on the cell membrane. This notion is in agreement with a well-established concept that elevated plasma PAI-1 levels, due mainly to obesity and insulin resistance, are risk factors for cardiovascular events.[45] Decreased amounts of tPA retained at the VEC surface because of an excess of PAI-1 in plasma are one possible mechanism of hypofibrinolysis under pathological conditions.

As well as their ability to secrete tPA, VECs perform a variety of functions that regulate vascular tone, coagulation, fibrinolysis, and inflammation. VEC dysfunction is characterized by vasoconstriction, thrombus formation, impaired fibrinolysis, and expression of adhesion molecules. Oliver et al reviewed[9] the complexity of vascular biology in VEC dysfunction and concluded that some conditions associated with reduced tPA release are not necessarily accompanied by impaired endothelium-dependent vasodilation. They also discuss the possibility that under certain circumstances, reduced tPA release may be a more sensitive marker of endothelial dysfunction than endothelium-dependent vasomotion, for example in smokers and patients with hypertension. To date, tPA release is recognized only by an increase in tPA concentration in plasma. However, tPA retention time on the cell surface, defined here as $T_{F1/2}$, would reflect fibrinolytic potency more directly than plasma tPA, and might also be an important indicator of VEC function. Evaluating tPA retention time in controlled secretion induced by various agonists including shear stress will be required to verify its significance for VEC function.

Acknowledgments

This work was supported by a Grant-in-Aid for Scientific Research (C: 19590858 [Y.S.]) and (C: 18590204 [T.U.]) from the Japan Society for the Promotion of Science (JSPS), a Japan Heart Foundation Research Grant (Y.S.), a grant from the Smoking Research Foundation (T.U.), and a grant from the Inamori Foundation (Y.S.).

Authorship

Contribution: Y.S. designed the study, performed the experiments, and wrote the paper; H.M. and H.I. performed research; and T.U. designed the study and edited the paper.

Conflict-of-interest disclosure: The authors declare no competing financial interests.

Correspondence: Yuko Suzuki, 1-20-1, Handa-yama, Higashi-ku, Hamamatsu, 431-3192, Japan; e-mail: seigan@hama-med.ac.jp.

References

1. Collen D, Lijnen HR. Basic and clinical aspects of fibrinolysis and thrombolysis. Blood. 1991;78:3114-3124.
2. Urano T, Sakakibara K, Rydzewski A, Urano S, Takada Y, Takada A. Relationships between euglobulin clot lysis time and the plasma levels of tissue plasminogen activator and plasminogen activator inhibitor 1. Thromb Haemost. 1990;63:82-86.
3. Urano T, Sumiyoshi K, Pietraszek MH, Takada Y, Takada A. PAI-1 plays an important role in the expression of t-PA activity in the euglobulin clot lysis by controlling the concentration of free t-PA. Thromb Haemost. 1991;66:474-478.
4. Ridker PM, Brown NJ, Vaughan DE, Harrison DG, Mehta JL. Established and emerging plasma biomarkers in the prediction of first atherothrombotic events. Circulation. 2004;109:IV6-IV19.

5. Wiman B, Andersson T, Hallqvist J, Reuterwall C, Ahlbom A, deFaire U. Plasma levels of tissue plasminogen activator/plasminogen activator inhibitor-1 complex and von Willebrand factor are significant risk markers for recurrent myocardial infarction in the Stockholm Heart Epidemiology Program (SHEEP) study. Arterioscler Thromb Vasc Biol. 2000;20:2019-2023.
6. Nordenhem A, Leander K, Hallqvist J, de Faire U, Sten-Linder M, Wiman B. The complex between tPA and PAI-1: risk factor for myocardial infarction as studied in the SHEEP project. Thromb Res. 2005;116:223-232.
7. Kolev K, Machovich R. Molecular and cellular modulation of fibrinolysis. Thromb Haemost. 2003;89:610-621.
8. Tachias K, Madison EL. Converting tissue-type plasminogen activator into a zymogen. J Biol Chem. 1996;271:28749-28752.
9. Oliver JJ, Webb DJ, Newby DE. Stimulated tissue plasminogen activator release as a marker of endothelial function in humans. Arterioscler Thromb Vasc Biol. 2005;25:2470-2479.
10. Newby DE, McLeod AL, Uren NG, et al. Impaired coronary tissue plasminogen activator release is associated with coronary atherosclerosis and cigarette smoking: direct link between endothelial dysfunction and atherothrombosis. Circulation. 2001;103:1936-1941.
11. Pretorius M, Rosenbaum DA, Lefebvre J, Vaughan DE, Brown NJ. Smoking impairs bradykinin-stimulated t-PA release. Hypertension. 2002;39:767-771.
12. Ridderstråle W, Ulfhammer E, Jern S, Hrafnkelsdottir T. Impaired capacity for stimulated fibrinolysis in primary hypertension is restored by antihypertensive therapy. Hypertension. 2006;47:686-691.
13. Kooistra T, Schrauwen Y, Arts J, Emeis JJ. Regulation of endothelial cell t-PA synthesis and release. Int J Hematol. 1994;59:233-255.
14. van den Eijnden-Schrauwen Y, Kooistra T, de Vries RE, Emeis JJ. Studies on the acute release of tissue-type plasminogen activator from human endothelial cells in vitro and in rats in vivo: evidence for a dynamic storage pool. Blood. 1995;85:3510-3517.
15. van den Eijnden-Schrauwen Y, Atsma DE, Lupu F, de Vries RE, Kooistra T, Emeis JJ. Involvement of calcium and G proteins in the acute release of tissue-type plasminogen activator and von Willebrand factor from cultured human endothelial cells. Arterioscler Thromb Vasc Biol. 1997;17:2177-2187.
16. Stein CM, Brown N, Vaughan DE, Lang CC, Wood AJ. Regulation of local tissue-type plasminogen activator release by endothelium-dependent and endothelium-independent agonists in human vasculature. J Am Coll Cardiol. 1998;32:117-122.
17. Knop M, Gerke V. Ca2+-regulated secretion of tissue-type plasminogen activator and von Willebrand factor in human endothelial cells. Biochim Biophys Acta. 2002;1600:162-167.
18. Emeis JJ, van den Eijnden-Schrauwen Y, van den Hoogen CM, de Priester W, Westmuckett A, Lupu F. An endothelial storage granule for tissue-type plasminogen activator. J Cell Biol. 1997;139:245-256.
19. Lang T, Wacker I, Steyer J, et al. Ca2+-triggered peptide secretion in single cells imaged with green fluorescent protein and evanescent-wave microscopy. Neuron. 1997;18:857-863.
20. Tsuboi T, Zhao C, Terakawa S, Rutter GA. Simultaneous evanescent wave imaging of insulin vesicle membrane and cargo during a single exocytotic event. Curr Biol. 2000;10:1307-1310.
21. Taraska JW, Perrais D, Ohara-Imaizumi M, Nagamatsu S, Almers W. Secretory granules are recaptured largely intact after stimulated exocytosis in cultured endocrine cells. Proc Natl Acad Sci U S A. 2003;100:2070-2075.
22. Imai Y, Matsushima Y, Sugimura T, Terada M. A simple and rapid method for generating a deletion by PCR. Nucleic Acids Res. 1991;19:2785.
23. de Vries C, Veerman H, Pannekoek H. Identification of the domains of tissue-type plasminogen activator involved in the augmented binding to fibrin after limited digestion with plasmin. J Biol Chem. 1989;264:12604-12610.
24. Edgell CJ, McDonald CC, Graham JB. Permanent cell line expressing human factor VIII-related antigen established by hybridization. Proc Natl Acad Sci U S A. 1983;80:3734-3737.
25. Emeis JJ, Edgell CJ. Fibrinolytic properties of a human endothelial hybrid cell line (Ea.hy 926). Blood. 1988;71:1669-1675.
26. Hecke A, Brooks H, Meryet-Figuiere M, et al. Successful silencing of plasminogen activator inhibitor-1 in human vascular endothelial cells using small interfering RNA. Thromb Haemost. 2006;95:857-864.
27. Urano T, Strandberg L, Johansson LB, Ny T. A substrate-like form of plasminogen-activator-inhibitor type 1: conversions between different forms by sodium dodecyl sulphate. Eur J Biochem. 1992;209:985-992.
28. Mogami H, Zhang H, Suzuki Y, et al. Decoding of short-lived Ca2+ influx signals into long term substrate phosphorylation through activation of two distinct classes of protein kinase C. J Biol Chem. 2003;278:9896-9904.
29. Suzuki Y, Zhang H, Saito N, Kojima I, Urano T, Mogami H. Glucagon-like peptide 1 activates protein kinase C through Ca2+-dependent activation of phospholipase C in insulin-secreting cells. J Biol Chem. 2006;281:28499-28507.
30. Urano T, Nagai N, Matsuura M, Ihara H, Takada Y, Takada A. Human thrombin and calcium bound factor Xa significantly shorten tPA-induced fibrin clot lysis time via neutralization of plasminogen activator inhibitor type 1 activity. Thromb Haemost. 1998;80:161-166.
31. Perrais D, Kleppe IC, Taraska JW, Almers W. Recapture after exocytosis causes differential retention of protein in granules of bovine chromaffin cells. J Physiol. 2004;560:413-428.
32. Tsuboi T, McMahon HT, Rutter GA. Mechanisms of dense core vesicle recapture following "kiss and run" ("cavicapture") exocytosis in insulin-secreting cells. J Biol Chem. 2004;279:47115-47124.
33. Taraska JW, Almers W. Bilayers merge even when exocytosis is transient. Proc Natl Acad Sci U S A. 2004;101:8780-8785.
34. Lochner JE, Honigman LS, Grant WF, et al. Activity-dependent release of tissue plasminogen activator from the dendritic spines of hippocampal neurons revealed by live-cell imaging. J Neurobiol. 2006;66:564-577.
35. Matsushita K, Morrell CN, Cambien B, et al. Nitric oxide regulates exocytosis by S-nitrosylation of N-ethylmaleimide-sensitive factor. Cell. 2003;115:139-150.
36. Lowenstein CJ, Morrell CN, Yamakuchi M. Regulation of Weibel-Palade body exocytosis. Trends Cardiovasc Med. 2005;15:302-308.
37. Fu J, Naren AP, Gao X, Ahmmed GU, Malik AB. Protease-activated receptor-1 activation of endothelial cells induces protein kinase Calpha-dependent phosphorylation of syntaxin 4 and Munc18c: role in signaling p-selectin expression. J Biol Chem. 2005;280:3178-3184.
38. Romani de Wit T, Rondaij MG, Hordijk PL, Voorberg J, van Mourik JA. Real-time imaging of the dynamics and secretory behavior of Weibel-Palade bodies. Arterioscler Thromb Vasc Biol. 2003;23:755-761.
39. Hannah MJ, Skehel P, Erent M, Knipe L, Ogden D, Carter T. Differential kinetics of cell surface loss of von Willebrand factor and its propolypeptide after secretion from Weibel-Palade bodies in living human endothelial cells. J Biol Chem. 2005;280:22827-22830.
40. Kranenburg O, Bouma B, Kroon-Batenburg LM, et al. Tissue-type plasminogen activator is a multiligand cross-beta structure receptor. Curr Biol. 2002;12:1833-1839.
41. Ichinose A, Takio K, Fujikawa K. Localization of the binding site of tissue-type plasminogen activator to fibrin. J Clin Invest. 1986;78:163-169.
42. Roda O, Chiva C, Espuna G, et al. A proteomic approach to the identification of new tPA receptors in pancreatic cancer cells. Proteomics. 2006;6(suppl 1):S36-S41.
43. Hajjar KA, Krishnan S. Annexin II: a mediator of the plasmin/plasminogen activator system. Trends Cardiovasc Med. 1999;9:128-138.
44. Kwaan HC, Wang J, Weiss I. Expression of receptors for plasminogen activators on endothelial cell surface depends on their origin. J Thromb Haemost. 2004;2:306-312.
45. Juhan-Vague I, Alessi MC. PAI-1, obesity, insulin resistance and risk of cardiovascular events. Thromb Haemost. 1997;78:656-660.